International Dairy Journal 92 (2019) 50–58

Contents lists available at ScienceDirect

International Dairy Journal

journal homepage: www.elsevier.com/locate/idairyj

Application of NIR spectroscopy and image analysis for the characterisation of grated Parmigiano-Reggiano cheese

Marcello Alinovi [a, *], Germano Mucchetti [a], Flavio Tidona [b]

[a] Department of Food and Drug, University of Parma, Parco Area delle Scienze 47/A, 43124, Parma, Italy
[b] Centro di Ricerca Zootecnia e Acquacoltura (CREA-ZA), via Lombardo 11, 26900, Lodi, Italy

ARTICLE INFO

Article history:
Received 4 December 2018
Received in revised form
7 January 2019
Accepted 9 January 2019
Available online 30 January 2019

ABSTRACT

Grated Parmigiano–Reggiano cheese holds a valuable market segment and its quality strictly depends on the amount of rind, size, shape of cheese particles and original cheese properties. Textural properties of the rind and inner part of the cheese significantly affect size and shape of grated particles. Rind produces a higher amount of finer and less circular particles than the inner region. Rind content established by European regulation (maximum 18%) is a major issue and could be successfully predicted by multivariate models developed on near-infrared (NIR) spectra. Image analysis (IA) was a suitable method to estimate rind percentage that was found positively correlated to number of particles, total surface covered by particles and circularity. IA and NIR spectroscopy enabled characterisation of the distribution of the particle in dimensional classes and could be used to control the maximum limit of 25% of particles finer than 0.5 mm provided by European regulation.

1. Introduction

Cheese rind of a long-ripened cheese has chemical and physical characteristics different from those of the other parts of the cheese as it is exposed during ripening to environmental conditions (i.e., air, water vapour pressure, light; surface microorganisms, sodium chloride) that contribute to differently modify the initial properties of the cheese matrix. The more evident changes for long-ripened cheeses without a specific surface microbiota are the decrease of moisture content and water activity, and the consequent decrease of proteolytic activities catalysed by indigenous proteinases (Cattaneo et al., 2008; Mayer, 1996). Furthermore, the prolonged contact with air and light increase the degree of oxidation (Karoui, Dufour, & De Baerdemaeker, 2007).

These phenomena can impact on the sensory perception of the rind, that is generally characterised by sensorial properties different from those of the inner part of the cheese, as evidenced by the presence of odour and flavour of "rind" among the descriptors of cheese sensory attributes (Biasioli et al., 2006; Zanoni, 2010).

Industrially, hard long-ripened cheese wheels are brushed and/or washed and then are either sliced to be sold in portions with or without rind or are further processed by grating. The market of cheese portions without rind created the availability of large amount of rind with a lower value that can be either sold separately as is or grated with other trimmed pieces of cheese and/or whole wheels. As the presence of excessive amounts of rind in grated cheese can be perceived by the consumer and can have a negative impact on the sensory characteristics (Zannoni & Hunter, 2015), the quality of grated cheese depends both on the original properties of the whole cheese and on the percentage of rind. In this context, some grated cheese produced under the rules of European Protected Designation of Origin (PDO) must comply with specific limitation regarding the presence and percentage of rind (e.g., Grana Padano, Parmigiano-Reggiano, Pecorino Sardo; Door, 2018).

Parmigiano–Reggiano (P–R) is a cooked, long-ripened, hard cheese made in Northern Italy registered as a PDO in the European Union (European Regulation No. 1151/2012; EU, 2012). The PDO status of P-R cheese is extended to the grated type, with grating and packaging operations that must take place in the same area of origin as that of production. Grated P-R cheese accounted for 13.5% of the overall market of P-R cheese in 2017 (+5.2% compared with 2016) and this percentage continuously increased in the last years (Parmigiano-Reggiano Consortium, 2017). PDO designation is restricted to grated cheeses accounting specific technical parameters, such as minimum 12 months of ripening, fat content not less than 32% in proportion to dry matter and moisture between 25%

* Corresponding author. Tel.: +39 0521 905950
E-mail address: marcello.alinovi@studenti.unipr.it (M. Alinovi).

https://doi.org/10.1016/j.idairyj.2019.01.010
0958-6946/

and 35%. Additionally, the aspect should be homogeneous, with less than 25% (without specifying if % is in weight or in volume) of particles having diameter less than 0.5 mm, and a quantity of rind less than 18% (w/w); rind is defined by the regulation as the external part of the cheese with a depth of 6 mm (Door, 2018). To date, no official analytical methods for the quantification of rind and finer particles are considered by the PDO regulation. The limit of 18% of rind in grated cheese can be surpassed because of process issues (e.g., mixing errors before grating when both whole wheels and trimmed parts are used or during packaging operations) or because of fraudulent reasons.

Particle size properties are an important issue in the quality control of food industries since they can affect texture, mouthfeel and further processing of products. The main techniques employed to measure particle size range from traditional sieving to sedimentation and light scattering; to this purpose, the use of image analysis (IA) has proven to be a valid alternative (Brosnan & Sun, 2004; Caccamo et al., 2004; Febbi, Menesatti, Costa, Pari, & Cecchini, 2015; Iezzi et al., 2012; Sugimoto, Hashimoto, Fukuike, Kodama, & Minagi, 2014), also thanks to the evolution and diffusion of high resolution digital machines. In particular, IA measurements have also been proposed to measure particle size properties of shredded cheese samples (Ni & Guansekaran, 2004). Studies in literature reported also the relation between product hardness and particle size resulting from wheat milling processes (Campbell, Fang, & Muhamad, 2007; Fang & Campbell, 2003).

In contrast, no literature data were found on the relation between textural and particle size properties of grated cheese. Concerning the detection of uncontrolled amount of rind in long ripened grated cheeses, analytical procedures range from chemical methods (Cattaneo et al., 2008) to NMR techniques (Shintu & Caldarelli, 2005), capacitive techniques (Cevoli et al., 2015), waveguide spectroscopy (Cevoli, Ragni, Gori, Berardinelli, & Caboni, 2012) and near-infrared spectroscopy (NIR) approaches (Barzaghi et al., 2016; Cevoli, Gori et al., 2013; Cevoli, Fabbri, Gori, Caboni, & Guarnieri, 2013; Musi & Filippi, 2015). NIR has also been applied as a good and fast alternative for particle size measurements of lactose monohydrate particles and wheat flour (Frake et al., 1998; Zhu, Xing, Lu, Huang, & Ng, 2017). Among other several analytical approaches in food science, NIR offers an interesting option of investigation: it does not require solvents or sample preparation and the same sample can be employed for other analytical tests. Moreover, the performance of diffuse reflectance analysis could be improved by using an integrating sphere in case of not homogeneous solid foods, especially when the sample is reduced in powder (Subramanian & Rodriguez-Saona, 2009). Overall costs are low and analysis times are very short if compared with traditional analytical approaches.

Considering the limitation imposed by PDO regulation and the risk of quality loss when an excessive amount of rind is present in the grated product, P-R dairies need fast and reliable methods to control their process conditions and to verify that grated cheese complies with both legal limits and with their quality programs. The aims of this work were to study how differences of texture and moisture content of P-R cheese can affect the particle size of grated cheese and to set up rapid methods based on IA and NIR techniques to measure the particle size and the quantity of rind present in grated P-R cheese.

2. Materials and methods

2.1. Sample collection and preparation

Cheese samples were collected from 3 cheese plants producing PDO Parmigiano-Reggiano (P-R) and supplied by Nuova Castelli Spa (Reggio Emilia, Italy), in portions of about 1 kg, packaged under vacuum and stored at 4 °C until use. Samples were chosen among 5 cheese batches with 5 different ripening times (12, 18, 21, 24 and 30 months) to represent the variability of available P-R cheeses processed by the grater. Portions of cheese to be analysed by texture analysis and moisture content did not need further preparation and were stored as a whole. For the preparation of grated samples, the rind of each cheese was cut at 6 mm of depth, according to the definition of rind provided by the PDO regulation and it was kept separately; the section between 6 mm and 20 mm of depth was removed, whereas the inner part of the cheese was taken as a whole. The rind and the cheese were separately grated by means of an electrically driven grater (Ardes AR7300, Milan, Italy) at Centro di Ricerca Zootecnia e Acquacoltura (CREA-ZA, Lodi, Italy). Pure grated inner part and rind samples were also analysed by IA to find out possible relations with textural properties and moisture content.

Table 1
Number of grated Parmigiano-Reggiano cheese samples analysed by near-infrared (NIR) spectroscopy and image analysis (IA) reported for every ripening time and rind percentage level considered in this study.[a]

Percentage (w/w)	Ripening time (months)	Number of samples analysed	
		NIR	IA
0	12, 18, 21, 24, 30	11	10
4	12, 24, 30	5	–
5	13, 21,24	4	–
9	12, 18, 21, 24, 30	18	10
10	12, 24, 30	9	–
15	13, 21, 24	4	–
16	12, 24, 30	5	–
18	12, 18, 21, 24, 30	18	10
20	12, 24, 30	9	–
25	13, 21, 24	4	–
27	12, 18, 21, 24, 30	18	10
30	12, 24, 30	8	–
36	12, 18, 21, 24, 30	18	10

[a] Percentage is percentage of rind of the sample (w/w); ripening time is of sampled rind and inner part.

To prepare samples to be analysed with NIR and IA, various mixtures of grated rind and grated inner part of cheeses were combined in different proportions and then accurately manually mixed into plastic bags. To simulate the wide variability occurring in industrial plants where whole wheels or pieces of cheese with different ages (rind and cheese) are grated, samples were combined at different ratios. The presence of different amounts of rind was set from 0 to 36% (w/w) for a total of 13 different percentages of rind (Table 1). Samples were stored at 4 °C. In total, 131 samples were analysed by NIR for the determination of the percentage of rind. Out of the 131 samples of the entire dataset, 50 samples were analysed by IA to build-up a partial least square (PLS) model for the quantification of cheese rind based on particle size measurements and a model for the determination of particle size properties based on NIR data.

2.2. Application of NIR in a P-R cheese grating industry

The best built-up NIR-PLS model was employed to evaluate the content of rind detected during filling and packaging operations at an industrial scale. P-R cheeses ripened 28 ± 2 months were grated using an industrial grater (Model HP 20, Cavecchi Srl, Reggio Emilia, Italy) to produce, in total, seven batches of grated cheese: each batch was monitored at six fixed production times (T0, T1, T2, T3, T4 and T5 min), collecting a package of 200 g of grated cheese from the

packaging line. Cheese batches to be grated were composed by trimmed pieces of cheese of various dimensions. Before processing, the grating system was cleaned to remove any residue derived from the previous batch. The collected samples were stored at 4 °C until they were analysed. Results are expressed as the mean of 4 measurements.

2.3. Analytical methods

2.3.1. NIR spectra acquisition of grated cheese samples

NIR spectra were acquired by a FT-NIR Tango spectrometer (Bruker, MA, USA) in the spectral range of 1000–2500 nm, recording 32 scans acquired with a resolution of 8 cm^{-1} as reported by Barzaghi et al. (2016). Samples were equilibrated at 25 ± 1 °C for about 1 h before analysis, mixed thoroughly and an amount of 25 g was loaded into a 95 mm diameter glass Petri plate. Each sample was analysed in duplicate. Additionally, each sample was subjected to a further grinding (treated samples) by means of a blender (Osterizer model 890-48H) for 30 s, and then reanalysed in duplicate to increase model robustness against light scattering phenomena. To develop models for rind quantification, both spectra of untreated and treated samples were considered and averaged. To create predictive models based on particle size parameters, only spectra of untreated samples were considered and averaged.

2.3.2. Image analysis

Images of grated cheese samples (0.21 × 0.30 m A4 scanner size) were acquired using a Hewlett Packard Scanjet 8200 scanner (Palo Alto, CA, USA) with a resolution of 600 dpi (corresponding to 236 pixels cm^{-1}) and saved in TIFF format. To avoid saturation effects and overlapping of particles, 0.3 g of grated cheese was preliminary tested as a suitable amount of sample to be carefully spread on a transparent paper to achieve a homogenous distribution. A black background was used to enhance contrast of acquired images; a graph paper was always included during image acquisition to set the scale, expressed in mm. Elaboration of the images was performed by using ImageJ software (National Institutes of Health, Gaithersburg, MD, USA); images were first turned into greyscale (8 bit) and then segmented into binary images using default algorithm, imposing threshold limits of 20 and 255 for the black background. Blanks of transparent paper (without samples) were also analysed and to avoid the interference of dusts, the command "Open" that performs an erosion operation followed by dilation, was applied to remove pixels of undefined objects not related to cheese particles.

The following parameters were taken into account: total number of particles (n) and total surface covered by particles (S_T) by 0.3 g of sample, circularity (C), Feret diameter (F) and minimum Feret diameter (mF). Feret diameter is defined as the diameter of the object connecting perpendicularly two parallel tangential lines restricting the object; it represents the diameter of the object along a specified direction. F and mF are often used as the dimensions of the particles (Febbi et al., 2015). To study the dimensional frequency distribution of the particles, 4 size classes were identified based on F and mF diameters, namely $F_{(<0.5\ mm,\ 0.5–1\ mm,\ 1–2\ mm,\ >2\ mm)}$ and $mF_{(<0.5\ mm,\ 0.5–1\ mm,\ 1–2\ mm,\ >2\ mm)}$. Each sample was analysed in triplicate.

2.3.3. Textural analysis

The textural properties of P-R cheese were measured according to the puncture test proposed by Breuil and Meullenet (2001) using a TA. XTplus Texture Analyzer (Stable Micro Systems, Godalming, UK) equipped with a 30 kg load cell and a stainless steel cylindrical probe with a 3 mm diameter (SMS P/3, Stable Micro Systems). Measurements were conducted at 0.8 mm s^{-1} with a trigger force of 5 g until a 10 mm distance was reached; pre-test and post-test speeds were set at 1 mm s^{-1}. Hardness at rupture (H_r), distance at rupture (D_r) and initial slope (S_{ini}) were respectively defined as the positive force value (N) and the distance (mm) at which sample showed rupture of its surface (the first peak originated during the puncture cycle) and the slope of the tangent until 0.5 s from the beginning of the analysis. Maximum hardness (H_{max}), distance at maximum force (D_{max}), positive work area (A_p) were respectively defined as the maximum positive force (N), distance to reach maximum force (mm) and the total positive work (N mm); Mod_1 was defined as the modulus (unitless) of the vector between the origin and the maximum force of the puncture graph. Texture was evaluated in different zones of the cheese wheel, namely inner part, underrind (portion of cheese between 6 mm and 20 mm of depth from the outer part of the wheel), and rind of the cheeses at different ageing times. Puncture tests of rind section exhibited H_r and D_r that coincided with H_{max} and D_{max} for all samples. Samples were equilibrated at 25 °C for 24 h prior to being analysed and reported measures were averages of six replicates.

2.3.4. Moisture content

Moisture content of cheeses was measured by drying samples at 102 °C (AOAC, 1990) until a constant weight was reached. Measures were done in triplicate in the same zones of cheeses (rind, underrind and inner part of the cheese) sampled for the texture analysis.

2.4. Data processing

2.4.1. Multivariate data processing

Principal component analysis (PCA) was applied as an exploratory analysis to observe a possible classification among samples with different rind percentages. To build up chemometric models of rind and particle size parameters' quantification, PLS regression technique (SIMPLS algorithm) was chosen and performed on NIR absorbance spectra and IA parameters of grated cheeses. PLS regression is a multivariate technique used to build predictive models when independent variables (spectral data, X-array) are many and collinear (Menesatti et al., 2010). This regression technique applies variables decomposition to reduce the quantity of given information by spectral data and image analysis parameters, relating X-array to a Y-vector (response variable). The result is the creation of a number of latent variables (LVs) that are a reconstruction of the original spectral data and that are highly correlated with the Y-response.

Different pre-processing transformations of absorbance spectra and IA parameters were evaluated (mean and median centering, auto-scaling, baseline correction, detrending, multiplicative scattering correction, extended multiplicative scattering correction, standard normal variate, Savitzky–Golay 1st-2nd derivative, generalised least squares weighting).

Cross-validation techniques (random sub-set, leave-one-out) were used to assess the best pre-processing method and to select the optimal number of LVs, by considering the root mean square error in cross validation (RMSECV) and the coefficient of determination (R^2). In addition, the root-mean-square error of calibration (RMSEC) was included in the calibration statistics to assess model goodness (Niu et al., 2008). For IA PLS model, variable importance in the projection (VIP) scores that express the importance of each variable in the definition of model's LVs (Gerretzen et al., 2016) were calculated according to Eq. (1):

$$VIP_k = \sqrt{K \sum_{f=1}^{f} \frac{w_{kf}^2 \cdot SSY_f}{SSY_t}} \quad (1)$$

where K is the total number of X parameters, w_{jf} is the weight value for *kth* parameter and *fth* latent variable, SSY_f is the sum of squares of explained variance by *kth* parameter for *fth* component and SSY_t is the total sum of squares explained of the dependent variable.

The calibration model developed based on rind quantification was finally validated to predict the percentage of rind of the samples in an independent testing set (prediction set). To perform validation, samples were divided prior to calibration into a calibration set (66%) and a prediction set (34%) based on Kennard–Stone sampling algorithm (Kennard & Stone, 1969). Because of the lower number of samples, models based on particle size parameters were not externally validated. All multivariate analyses were performed using PLS Toolbox v. 8.0 (Eigenvector Research Inc., WA, USA) with MATLAB V8.5.0 R15a (The Math Works, Natick, MA, USA).

2.4.2. Statistical analyses

Two-way analysis of variance (ANOVA) was performed to assess statistical differences based on textural, particle size and moisture data as function of different ages and zones in cheese geometry or percentages of rind. Univariate statistical analyses were carried out using PRC GLM of SAS (SAS Inst. Inc., NC, USA); least squares means with LSD adjustment was used to perform multiple comparisons among means. Pearson correlation coefficients were calculated among the measured parameters using SPSS v.25.0 (SPSS Inc., Armonk, USA). Before statistical procedures, data to be analysed were tested for normality and homogeneity of variance.

3. Results and discussion

3.1. Relationships among textural properties, moisture content and particle size

Samples showed clear differences in textural properties among different zones of the cheese. As expected, rind showed greater hardness at rupture (H_r), maximum hardness (H_{max}), positive work area (A_p), initial slope (S_{ini}) and modulus (Mod_1) than underrind and inner part of the cheese (Table 2); underrind was slightly harder than inner part of the cheese although H_r, H_{max} values were not significantly different for almost all the comparisons.

The inverse relation between moisture content and hardness has already been shown for parmesan-type cheeses (Jaster et al., 2014), but was not yet investigated for different zones of the cheese wheel. A higher firmness of cheese rind than the inner part of the cheese is related to the highly different moisture content of the zones of the cheese; in facts, the mean difference of moisture content between the inner and the rind part of the cheese was 14.01 ± 1.98%. Differences of moisture between the inner and the outer zones of the wheel may also affect bacterial growth and biochemical reactions leading to different sensory properties among different cheese zones (Cattaneo et al., 2008; Lindner et al., 2008; Malacarne et al., 2009; Mayer, 1996). Consequently, texture may affect the result of grating operations in terms of dimension and shapes of the particles.

The rind showed higher values of distance at rupture (D_r) indicating that this zone was more elastic than the inner, which was found to be more brittle (Patel, Upadhyay, Miyani, & Pandya, 1993). Ripening time affects both textural and moisture content results and consequently H_r and moisture were strongly inversely related (Table 3). Despite a stronger texture and a lower moisture content is expected as the ripening time increases, this relation between time and cheese properties can be always true only for the same batch of cheese. In fact, in particular for outer cheese zones (rind and underrind), a high variability in textural properties and moisture content was observed among different ripening times and no clear relations were highlighted, likely due to the high variability in P-R cheeses that can be partially caused by the use of milk without standardised chemical composition and by dairy specificity practices according to P-R cheese-making technology (Mucchetti et al., 2014); for instance, samples at 18 and 24 months of ripening were found to be firmer and drier than samples at 12 and 21 months, respectively. Samples at 30 months were nearly two-times harder and drier than samples at 12 months.

Textural properties affected size and dimensions of the particles deriving from the grating procedure. Grated samples with different ripening time and percentages of rind (0, 18, 100%) showed differences in IA parameters, as reported in Table 4. Number of particles (n) and total surface covered by particles (S_T) present in the same amount of cheese (0.3 g) were highly positively influenced by rind

Table 2
Textural parameters and moisture content of Parmigiano-Reggiano cheese samples having different ripening times.[a]

Ripening time (months)	Wheel zone	H_r (N)	D_r (mm)	H_{max} (N)	D_{max} (mm)	S_{ini} (N mm^{-1})	Mod_1 (-)	A_p (N mm)	Moisture (%, w/w)
12	inner	4.03 ± 0.37 ^{e}	0.88 ± 0.11 ^{c}	5.60 ± 0.36 ^{ef}	9.94 ± 0.09 ^{a}	6.31 ± 1.36 ^{e}	11.41 ± 0.12 ^{f}	44.20 ± 3.05 ^{f}	32.00 ± 1.38 ^{a}
	underrind	6.78 ± 1.18 ^{de}	1.26 ± 0.15 ^{c}	9.65 ± 1.39 ^{def}	10.00 ± <0.01 ^{a}	10.03 ± 2.63 ^{de}	13.92 ± 1.01 ^{d}	76.39 ± 12.28 ^{ef}	26.67 ± 2.32 ^{cd}
	rind	36.68 ± 6.55 ^{c}	3.51 ± 0.42 ^{a}	36.68 ± 6.55 ^{c}	3.51 ± 0.42 ^{c}	22.45 ± 4.83 ^{c}	36.85 ± 6.52 ^{a}	295.45 ± 59.90 ^{cd}	18.05 ± 2.16 ^{fg}
18	inner	3.50 ± 0.39 ^{e}	1.19 ± 0.64 ^{c}	5.26 f ± 0.63 ^{f}	9.99 ± 0.02 ^{a}	5.54 ± 1.71 ^{e}	11.30 ± 0.30 ^{f}	40.45 ± 4.52 ^{f}	32.13 ± 0.33 ^{a}
	underrind	5.37 ± 1.32 ^{de}	1.23 ± 0.65 ^{c}	8.32 ± 1.67 ^{ef}	9.75 ± 0.6 ^{ab}	7.89 ± 2.97 ^{de}	12.88 ± 1.13 ^{de}	63.76 ± 12.41 ^{ef}	28.19 ± 0.93 ^{bc}
	rind	35.45 ± 8.10 ^{c}	3.58 ± 0.46 ^{a}	35.46 ± 8.10 ^{c}	3.63 ± 0.45 ^{c}	21.94 ± 5.12 ^{c}	35.66 ± 8.04 ^{a}	267.60 ± 70.12 ^{d}	20.57 ± 1.98 ^{ef}
21	inner	4.42 ± 0.45 ^{de}	1.20 ± 0.62 ^{c}	6.67 ± 0.58 ^{ef}	9.24 ± 1.84 ^{ab}	5.90 ± 3.45 ^{e}	11.45 ± 1.46 ^{e}	51.50 ± 3.25 ^{f}	31.46 ± 0.80 ^{ab}
	underrind	7.23 ± 1.19 ^{de}	1.14 ± 0.37 ^{c}	11.42 ± 1.93 ^{de}	9.46 ± 1.29 ^{ab}	12.50 ± 3.21 ^{de}	14.88 ± 1.81 ^{c}	89.45 ± 15.43 ^{e}	26.10 ± 2.22 ^{cd}
	rind	49.88 ± 8.67 ^{b}	3.75 ± 0.94 ^{a}	49.88 ± 8.67 ^{b}	3.75 ± 0.94 ^{c}	30.24 ± 10.86 ^{b}	50.04 ± 8.61 ^{a}	391.56 ± 70.34 ^{b}	15.27 ± 1.02 ^{gh}
24	inner	4.53 ± 0.71 ^{de}	1.03 ± 0.20 ^{c}	6.68 ± 0.37 ^{ef}	9.37 ± 1.50 ^{ab}	6.98 ± 2.76 ^{e}	11.57 ± 0.94 ^{e}	52.34 ± 2.30 ^{ef}	29.02 ± 1.64 ^{abc}
	underrind	6.33 ± 0.73 ^{de}	1.13 ± 0.6 ^{c}	10.86 ± 1.43 ^{de}	8.91 ± 2.14 ^{b}	9.75 ± 3.74 ^{de}	14.20 ± 1.19 ^{c}	84.56 ± 11.88 ^{ef}	27.07 ± 3.48 ^{c}
	rind	45.66 ± 6.79 ^{b}	3.47 ± 0.4 ^{a}	45.66 ± 6.79 ^{b}	3.47 ± 0.40 ^{c}	26.99 ± 3.42 ^{b}	45.79 ± 6.78 ^{a}	337.58 ± 62.09 ^{bc}	16.42 ± 2.07 ^{gh}
30	inner	5.58 ± 0.73 ^{de}	1.27 ± 0.51 ^{c}	8.87 ± 2.10 ^{ef}	9.76 ± 0.58 ^{ab}	7.43 ± 2.98 ^{de}	13.30 ± 1.17 ^{d}	66.24 ± 10.18 ^{ef}	29.59 ± 1.90 ^{abc}
	underrind	10.68 ± 2.59 ^{d}	2.19 ± 0.88 ^{b}	15.25 ± 3.18 ^{d}	9.99 ± 0.01 ^{a}	10.39 ± 3.19 ^{d}	18.29 ± 2.76 ^{b}	117.44 ± 25.10 ^{ef}	23.49 ± 2.17 ^{de}
	rind	61.02 ± 11.62 ^{a}	3.98 ± 0.60 ^{a}	61.02 ± 11.62 ^{a}	3.98 ± 0.60 ^{c}	38.42 ± 9.30 ^{a}	61.16 ± 11.57 ^{a}	483.37 ± 97.82 ^{a}	13.85 ± 1.13 ^{h}

[a] Textural parameters are: H_r, hardness at rupture; D_r, distance at rupture; H_{max}, maximum hardness; D_{max}, distance at maximum force; S_{ini}, initial slope; Mod_1, modulus between the origin and the maximum force; A_p, positive work area. Multiple comparisons were performed using GLM procedure with ls means option with LSD adjustment (SAS Institute, Cary, North Carolina). Results (mean ± standard deviation) are expressed for different zones of the cheese; means with different superscripts for each textural parameter considered (column) are statistically different ($P < 0.05$).

Table 3
Pearson correlation coefficients for particle size and textural parameters evaluated for rind and inner part of Parmigiano-Reggiano cheese samples.[a]

Parameter	D_r (mm)	Moisture (%, w/w)	n (-)	S_T (mm^2)	C (-)	$F_{<0.5mm}$ (%)	$F_{0.5-1mm}$ (%)	F_{1-2mm} (%)	$F_{>2mm}$ (%)	$mF_{<0.5mm}$ (%)	$mF_{0.5-1mm}$ (%)	mF_{1-2mm} (%)	$mF_{>2mm}$ (%)
H_r (N)	0.820**	−0.961**	0.934**	0.913**	−0.726**	0.794**	−0.869**	−0.652**	−0.083	0.765**	−0.811**	−0.592**	−0.460*
D_r (mm)		−0.886**	0.897**	0.909**	−0.711**	0.807**	−0.891**	−0.668**	−0.038	0.780**	−0.828**	−0.603**	−0.455*
Moisture (%, w/w)			−0.966**	−0.955**	0.774**	−0.849**	0.913**	0.727**	0.181	−0.828**	0.865**	0.679**	0.576*
n (-)				0.994**	−0.765**	0.900**	−0.941**	−0.778**	−0.183	0.884**	−0.922**	−0.719**	−0.581**
S_T (mm^2)					−0.796**	0.887**	−0.929**	0-0.766**	−0.178	0.879**	−0.915**	−0.717**	−0.589**
C (-)						−0.485**	0.609**	0.338	−0.135	0.518*	0.563**	0.356	0.312
$F_{<0.5mm}$ (%)							−0.935**	0-0.956**	−0.449*	0.987**	−0.991**	−0.895**	−0.736**
$F_{0.5-1mm}$ (%)								0.798**	0.121	−0.888**	0.942**	0.692**	0.496*
F_{1-2mm} (%)									0.630**	−0.974**	0.944**	0.966**	0.827*
$F_{>2mm}$ (%)										−0.520*	0.392*	0.753**	0.860**
$mF_{<0.5mm}$ (%)											−0.988**	−0.942**	−0.801**
$mF_{0.5-1mm}$ (%)												0.881**	0.709**
mF_{1-2mm} (%)													0.920**

[a] Abbreviations are: D_r, distance at rupture; n, total number of particles; S_T, total surface covered by particles; C, circularity; F, Feret diameter; mF, minimum Feret diameter; *$P < 0.05$, **$P < 0.001$.

Table 4
Image analysis parameters of Parmigiano-Reggiano grated cheese samples having different ripening times.[a]

Ripening time (months)	Rind (%, w/w)	n (-)	S_T (mm^2)	C (-)	$F_{<0.5mm}$ (%)	$F_{0.5-1mm}$ (%)	F_{1-2mm} (%)	$F_{>2mm}$ (%)	$mF_{<0.5mm}$ (%)	$mF_{0.5-1mm}$ (%)	mF_{1-2mm} (%)	$mF_{>2mm}$ (%)
12	0	1899 ± 78 ^{i}	631 ± 17 ^{h}	0.84 ± 0.01 ^{bc}	42.75 ± 1.59 ^{i}	38.76 ± 1.77 ^{a}	15.54 ± 0.87 ^{b}	2.95 ± 0.14 ^{c}	66.19 ± 1.3 ^{g}	27.50 ± 1.11 ^{b}	5.38 ± 0.58 ^{b}	0.93 ± 0.29 ^{b}
	18	4714 ± 292 ^{g}	1033 ± 10 ^{f}	0.83 ± 0.01 ^{cde}	53.72 ± 1.79 ^{efg}	32.27 ± 1.19 ^{ef}	11.48 ± 0.55 ^{de}	2.53 ± 0.33 ^{cde}	77.96 ± 1.08 ^{de}	18.67 ± 0.90 ^{cd}	2.99 ± 0.35 ^{de}	0.38 ± 0.08 ^{cd}
	100	18028 ± 881 ^{c}	2701 ± 217 ^{c}	0.83 ± 0.01 ^{cde}	65.47 ± 1.40 ^{a}	24.26 ± 0.80 ^{g}	8.05 ± 0.59 ^{h}	2.21 ± 0.30 ^{def}	87.50 ± 0.78 ^{a}	10.79 ± 0.49 ^{f}	1.55 ± 0.27 ^{g}	0.16 ± 0.07 ^{de}
18	0	881 ± 174 ^{i}	432 ± 33 ^{i}	0.85 ± 0.01 ^{b}	39.53 ± 2.70 ^{i}	36.18 ± 0.78 ^{bc}	18.67 ± 2.06 ^{a}	5.62 ± 0.88 ^{a}	59.30 ± 3.09 ^{h}	29.81 ± 1.80 ^{a}	8.90 ± 1.33 ^{a}	1.99 ± 0.45 ^{a}
	18	3306 ± 107 ^{h}	834 ± 14 ^{g}	0.82 ± <0.01 ^{ef}	51.06 ± 2.33 ^{g}	32.32 ± 2.08 ^{ef}	13.08 ± 0.4 ^{cd}	3.55 ± 0.39 ^{b}	77.08 ± 0.93 ^{e}	19.22 ± 1.14 ^{cd}	3.17 ± 0.22 ^{d}	0.53 ± 0.08 ^{c}
	100	17317 ± 187 ^{c}	2755 ± 35 ^{c}	0.82 ± <0.01 ^{f}	61.25 ± 0.22 ^{bc}	26.55 ± 0.53 ^{g}	9.46 ± 0.31 ^{gh}	2.75 ± 0.03 ^{cd}	85.42 ± 0.09 ^{ab}	12.47 ± 0.05 ^{f}	1.93 ± 0.07 ^{fg}	0.17 ± 0.01 ^{de}
21	0	3911 ± 75 ^{gh}	785 ± 57 ^{gh}	0.87 ± 0.01 ^{a}	56.15 ± 2.62 ^{def}	33.13 ± 1.61 ^{de}	9.56 ± 0.91 ^{gh}	1.16 ± 0.21 ^{ij}	79.34 ± 1.91 ^{de}	18.15 ± 1.47 ^{d}	2.22 ± 0.40 ^{efg}	0.29 ± 0.06 ^{cde}
	18	6865 ± 574 ^{e}	1203143 ^{e}	0.85 ± 0.01 ^{b}	58.68 ± 1.50 ^{cd}	30.20 ± 0.55 ^{f}	9.53 ± 1.34 ^{gh}	1.59 ± 0.25 ^{ghi}	83.02 ± 1.89 ^{bc}	15.16 ± 1.68 ^{e}	1.65 ± 0.23 ^{g}	0.18 ± 0.03 ^{de}
	100	19378 ± 881 ^{b}	2916 ± 143 ^{b}	0.82 ± 0.01 ^{f}	61.66 ± 3.50 ^{bc}	25.83 ± 1.93 ^{g}	9.68 ± 1.21 ^{fgh}	2.83 ± 0.37 ^{c}	85.44 ± 1.97 ^{ab}	12.34 ± 1.76 ^{f}	2.07 ± 0.17 ^{fg}	0.14 ± 0.04 ^{de}
24	0	3246 ± 320 ^{h}	834±5 ^{g}	0.85 ± 0.01 ^{b}	46.57 ± 4.02 ^{h}	37.70 ± 2.22 ^{ab}	14.12 ± 1.66 ^{bc}	1.61 ± 0.22 ^{ghi}	69.46 ± 3.11 ^{f}	25.89 ± 2.12 ^{b}	4.42 ± 0.99 ^{c}	0.23 ± 0.04 ^{de}
	18	6418 ± 101 ^{ef}	124361 ^{e}	0.84 ± 0.01 ^{bcd}	52.87 ± 1.36 ^{fg}	34.90 ± 0.95 ^{cd}	10.76 ± 0.89 ^{efg}	1.47 ± 0.08 ^{hi}	78.74 ± 1.58 ^{de}	18.94 ± 1.38 ^{cd}	2.23 ± 0.21 ^{efg}	0.09±<0.01 ^{e}
	100	19162 ± 953 ^{b}	2831 ± 135 ^{bc}	0.83 ± <0.01 ^{ef}	62.93 ± 0.89 ^{ab}	26.10 ± 0.55 ^{g}	8.94 ± 0.43 ^{h}	2.03 ± 0.04 ^{efg}	85.92 ± 0.52 ^{a}	12.37 ± 0.42 ^{f}	1.60 ± 0.08 ^{g}	0.12 ± 0.04 ^{e}
30	0	5805 ± 479 ^{f}	1129 ± 76 ^{ef}	0.85 ± <0.01 ^{b}	51.92 ± 2.97 ^{g}	35.92 ± 2.83 ^{bc}	11.25 ± 0.46 ^{ef}	0.91 ± 0.31 ^{j}	76.79 ± 1.69 ^{e}	20.57 ± 1.88 ^{c}	2.53 ± 0.20 ^{def}	0.11 ± 0.05 ^{e}
	18	9070 ± 717 ^{d}	1585 ± 66 ^{d}	0.83 ± <0.01 ^{cde}	56.83 ± 0.69 ^{de}	31.17 ± 0.57 ^{ef}	10.62 ± 0.17 ^{efg}	1.38 ± 0.17 ^{hij}	80.47 ± 0.76 ^{cd}	17.24 ± 0.65 ^{de}	2.20 ± 0.06 ^{efg}	0.10 ± 0.06 ^{e}
	100	22447 ± 1473 ^{a}	3184 ± 107 ^{a}	0.83 ± 0.01 ^{def}	64.94 ± 2.41 ^{ab}	24.70 ± 1.26 ^{g}	8.47 ± 0.86 ^{h}	1.89 ± 0.30 ^{fgh}	86.94 ± 1.33 ^{a}	11.28 ± 1.03 ^{f}	1.66 ± 0.25 ^{g}	0.12 ± 0.06 ^{e}

[a] Results (mean ± standard deviation) of total number of particles (n), total surface covered by particles (S_T), circularity (C), Feret diameter (F) and minimum Feret diameter (mF) are expressed as a function of the different rind percentage present in the samples. Multiple comparisons were performed using GLM procedure with least squares means option with LSD adjustment (SAS Institute, Cary, North Carolina). Means with different superscripts for each parameter considered (in columns) are statistically different ($P < 0.05$).

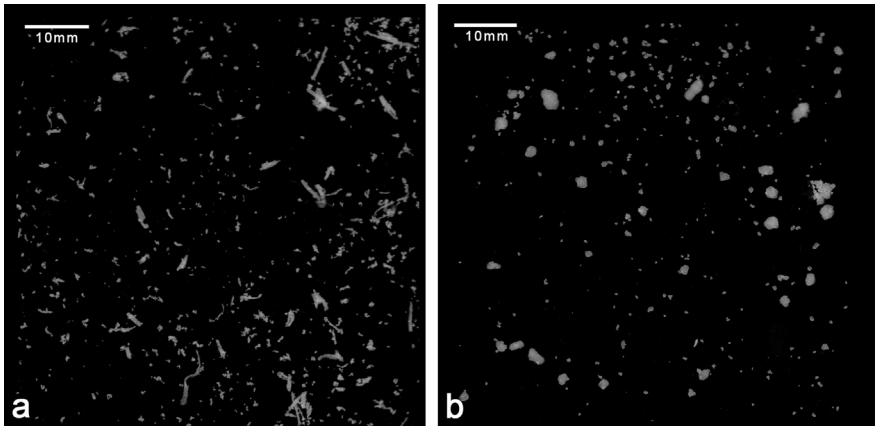

Fig. 1. Details of image acquired for rind (a) and inner part (b) of grated Parmigiano-Reggiano cheese after 24 months of ripening.

content. Grated rind fraction showed a largely higher amount of finer, small particles (F and mF < 0.5 mm) and consequently a lower number of larger particles (F and mF in the range between 0.5–1 mm and 1–2 mm).

Considering different ripening times, no clear trends were highlighted among samples as well as for textural parameters and moisture content; however, significantly strong positive correlations among n, S_T, $F_{<0.5\ mm}$, $mF_{<0.5\ mm}$ and H_r, D_r were observed. A negative correlation between the above-mentioned IA parameters and moisture content was also highlighted (Table 3). It has been reported in literature that a higher firmness can produce lower particle sizes as the result of grinding/grating operations in the case of wheat milling (Campbell et al., 2007; Fang & Campbell, 2003; Haddad, Mabille, Mermet, Abecassis, & Benet, 1999); in fact, the result of these operations could be affected by product hardness and moisture. Also, mean circularity (C) was slightly affected by grinded cheese zone although it was not always statistically different; grated rind showed lower circularity values than the inner part of the cheese and this is because rind's particles with F and mF bigger than 0.5 mm tends to be characterised by a more elongated, fibrous shape (Fig. 1).

3.2. PLS models development for the prediction of rind percentage and particle size properties

3.2.1. Rind percentage determination based on particle size measurements

Considering the different particle characteristics observed for rind and the inner part of the cheese (see paragraph above), PLS regression was performed to build up a quantitative model based on IA parameters for the determination of the rind content in grated cheese samples (Table 5). Autoscaling was chosen as pre-processing method; model resulted in 2 LVs that explained 87.22% and 87.81% of total variance for X- and Y-block, respectively. Calibration determination coefficient (R^2_{cal}) was 0.88, while cross-validation determination coefficient (R^2_{cv}) and RMSECV were 0.86 and 4.17%, respectively. Model's goodness of fit can be considered good (Karoui et al., 2006).

VIP scores (Fig. 2) showed that C, S_T, n, $F_{0.5–1\ mm}$, $F_{>2\ mm}$ were the most relevant variables having a score higher than 1, while the other mF and F parameters did not seem to be significant in determining the percentage of rind. Results highlighted a higher error than those reported by other authors with NIRs (Barzaghi

Table 5
Partial least squares regression results using cheese near infra-red (NIR) spectra and image analysis (IA) parameters to predict rind percentage and particle size properties of Parmigiano-Reggiano grated cheese samples.[a]

Data source	Model	Spectral range (nm)	Preprocessing method	Calibration data set			Calibration				Cross-validation		Validation		
				Range	Mean	SD	n	LVs	R^2	SEC	R^2	RMSECV	n	R^2	RMSEP
IA	RP (%, w/w)	–	Autoscale	–	–	–	50	2	0.880	3.90	0.860	4.17	–	–	–
NIR	RP (%, w/w)	1000–2500	1D + MSC + Autoscale	–	–	–	87	5	0.956	2.72	0.914	3.24	44	0.847	3.82
NIR	RP (%, w/w)	1064–1335; 1933–2357	1D + MSC + Autoscale	–	–	–	87	4	0.952	2.42	0.936	2.86	44	0.875	3.44
NIR	RP (%, w/w)	1000–2500	1D + SNV + Autoscale	–	–	–	87	5	0.952	2.38	0.925	3.00	44	0.858	3.69
NIR	RP (%, w/w)	1064–1335; 1933–2357	1D + SNV + Autoscale	–	–	–	87	4	0.952	2.41	0.934	2.89	44	0.874	3.45
NIR	n (-)	1000–2500	Mean centre	620–10743	5507	2510	46	1	0.851	969	0.828	1045	–	–	–
NIR	S_T (mm^2)	1000–2500	Autoscale	334–1731	1087	342	46	1	0.872	122	0.855	130	–	–	–
NIR	$F_{<0.5mm}$ (%)	1000–2500	Mean centre	34.93–64.76	52.55	7.16	46	1	0.607	4.49	0.497	5.15	–	–	–
NIR	$F_{0.5–1mm}$ (%)	1000–2500	Mean centre	26.70–43.71	33.53	4.14	46	2	0.602	2.61	0.504	2.94	–	–	–
NIR	$F_{1–2mm}$ (%)	1000–2500	Mean centre	7.53–20.05	11.64	2.96	46	3	0.615	1.84	0.510	2.10	–	–	–
NIR	$F_{>2mm}$ (%)	1000–2500	Mean centre	0.99–6.56	2.27	1.27	46	2	0.646	0.76	0.013	0.84	–	–	–
NIR	$mF_{<0.5mm}$ (%)	1000–2500	Mean centre	57.30–86.66	76.96	7.45	46	1	0.704	4.05	0.633	4.54	–	–	–
NIR	$mF_{0.5–1mm}$ (%)	1000–2500	Mean centre	12.01–34.50	19.57	5.29	46	2	0.682	2.98	0.583	3.44	–	–	–
NIR	$mF_{1–2mm}$ (%)	1000–2500	Mean centre	1.21–9.95	3.06	2.00	46	3	0.839	0.80	0.749	0.75	–	–	–
NIR	$mF_{>2mm}$ (%)	1000–2500	Mean centre	0.09–2.38	0.41	0.52	46	3	0.872	0.18	0.810	0.23	–	–	–

[a] Abbreviations are: RP, rind percentage; n, total number of particles; S_T, total surface covered by particles; F, Feret diameter; mF, minimum Feret diameter; 1D, 1st derivative (Savitzky–Golay); MSC, multiplicative scattering correction; SNV, standard normal variate; LVs, latent variables; R^2, coefficient of determination; SEC, square error of calibration; RMSEC, root-mean-square error in cross validation; RMSEP, root mean square error of prediction.

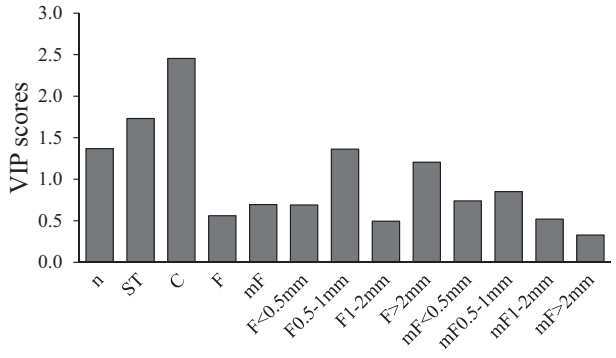

Fig. 2. Variable importance in the projection (VIP) scores of image analysis variables (n, total number of particles; S_T, total surface covered by particles; C, circularity; F, Feret diameter; mF, minimum Feret diameter) for the model built for the quantification of rind percentage in Parmigiano-Reggiano samples. The VIP scores shows the relative importance of each variable in the projection of model's LVs.

et al., 2016; Cevoli, Fabri et al., 2013; Musi & Filippi, 2015) but showed the feasibility of IA to be a fast and economic complementary analysis to detect the rind percentage in grated P-R cheese.

3.2.2. Preliminary analyses of NIR spectra

The effect of different rind percentages on NIR spectra of grated cheese samples is shown in Fig. 3a. Averaged raw spectra containing 4 different rind percentages (0, 9, 18, 27, 36%) of the whole dataset showed similar spectral behaviour and were characterised by the main absorption bands of water and fat (Cevoli, Gori et al., 2013). A decreasing baseline height of the spectrum was highlighted, as the rind content of the sample increases because of the increasing percentage of particles with lower dimensions (Holroyd, 2013; Silaghi, Giunchi, Fabbri, & Ragni, 2009). Moreover, a high difference in absorbance values was observed at water absorption wavelengths (1936 nm and 1457 nm); samples with a higher content of rind showed lower absorbance values because of their lower moisture content. Performing a first derivate on raw spectra (Fig. 3b), contributions from the lipids, water and proteins (bands located around 1885 nm and 2190 nm attributed to the water absorption in the 1st overtone and N–H and O–H bonds, respectively), as reported by other authors (Downey et al., 2005; Karoui et al., 2006), can be clearly observed.

Spectral differences were also investigated by PCA analysis to explore the effect of increasing amount of rind in the samples (Fig. 4a). Observing the scores plot graph, a good separation among samples with different rind percentages was highlighted; in particular, samples were greatly discriminated by PC 1, that explained 98.29% of the total variance among the samples.

3.2.3. Prediction of IA parameters based on NIR analysis

PCA scores plot of grated cheese NIR spectra showed a good separation among samples characterised by low and high number of particles (n) as shown in Fig. 4b. Moreover, a good discrimination of treated (further grinded) and untreated grated cheese samples was obtained with PCA scores plot (results not shown) as a consequence of light scattering phenomena (data not shown).

Considering the effect of light scattering over NIR spectra, PLS models for the prediction of particle size based on IA measurements were built up (Table 5). Models for the prediction of n and S_T parameters gave good results both in calibration and cross-validation, as R^2 were higher than 0.828; moreover, models were

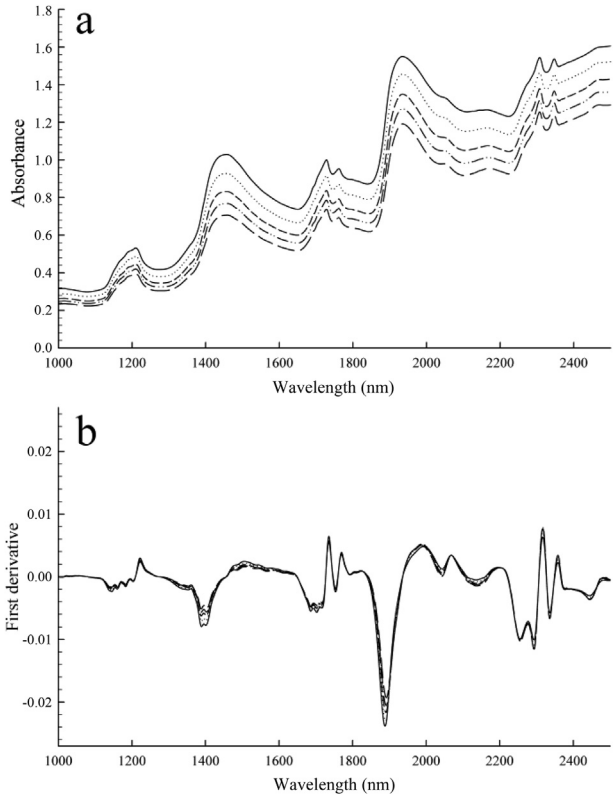

Fig. 3. Averaged raw spectra (a) and Savitzky–Golay first derivative (b) of grated cheese having different rind percentages (w/w), namely 0% (——), 9% (·····), 18% (- - - - -), 27% (— · ·), and 36% (— —).

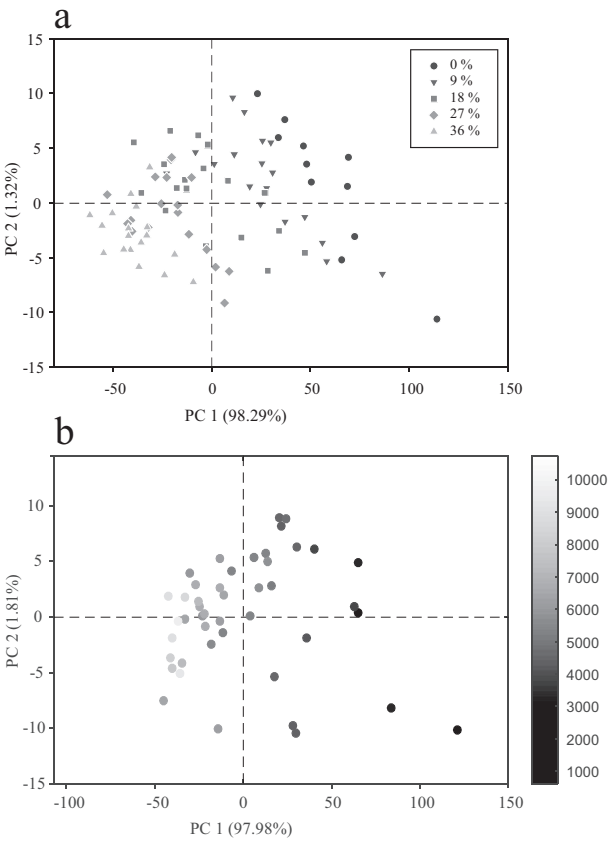

Fig. 4. Principal component analysis (PCA) scores plot of grated cheese samples having different rind percentages (w/w), namely 0% (●), 9% (▼), 18% (■), 27% (◆) and 36% (▲) (a), and characterised by a different number of particles in 0.3 g of sample (b).

considerably robust and stable as were constituted by only 1 latent variable that explained a large amount of response variance. Best preprocessing method of NIR spectra was mean centering and autoscaling of data for all particle size models, respectively. As expected, data pretreatment involving scattering correction (1st derivative, multiple scattering correction, baseline adjustment) gave worst results.

Models concerning frequency percentage estimation of F and mF at different class sizes (<0.5 mm, 0.5–1 mm, 1–2 mm, >2 mm) did not give good results, as R^2 was in the range between 0.5 and 0.7 both in calibration and cross-validation, with the exception of $mF_{>2\ mm}$ that gave a determination coefficient higher than 0.8; these reported results can be caused by a non-homogeneous distribution of y-values across the calibration range. Additionally, the ratio of prediction to deviation (RPD, not shown) of these models was lower than 2, except for $mF_{>2\ mm}$. Thus, models for the prediction of frequency percentages classes based on mF and F were able only to discriminate between low and high values (Karoui et al., 2006).

3.2.4. NIR analysis for the prediction of rind content

Concerning the prediction of rind with NIRs, data were preprocessed using 1st derivative, multiple scattering correction followed by autoscaling or 1st derivative, standard normal variate followed by autoscaling; the two different preprocessing procedures gave similar results (Table 5). Moreover, for each preprocessing method 2 different PLS models were built up: a model that processed the whole acquired NIR spectrum (1000–2500 nm) of the samples and a model based on the selection of a sub-region located in two wavelength intervals (1064–1335 nm, 1933–2357 nm) to reduce the complexity of PLS models and reach a desired error level (Jiang, Berry, Siesler, & Ozaki, 2002).

The selection of informative regions aims to further improve the prediction ability of the PLS models than those of the models constructed on the whole spectral points (Du, Liang, Jiang, Berry, & Ozaki, 2004). The excluded wavelength intervals mostly refer to water absorption IR bands that, in the case of P-R, can be subjected to fluctuations because of moisture content variability, that is influenced by cheesemaking and ripening conditions (Table 2). Indeed, the PLS models built up on the selected sub-region were more robust than models including the entire absorption spectrum, as they were constituted by 4 LVs instead of 5. R^2 values were higher than 0.93 in calibration and cross-validation while slightly decreased in validation (0.87). Taking into account the root mean square error of prediction (RMSEP) values (3.44–3.45%), performance of the models can be considered good and similar to that reported in literature (Barzaghi et al., 2016; Cevoli et al., 2012; Cevoli, Fabbri et al., 2013; Cevoli, Gowri et al., 2013).

3.3. Application of NIR model to predict the percentage of rind during industrial grating operations

A simple calculation of the volume ratio between the rind and the inner part of the whole cheese, considering the thickness of 6 mm of the rind and the variability of the dimension of the wheel that are established by PDO Regulation (diameter of the faces from 35 to 45 cm and heel height from 20 to 26 cm), shows that this ratio is largely less than 18% also for the smallest wheel. Thus, the limit of 18% of rind in grated cheese can be surpassed because of mixing errors before grating when both whole wheels and trimmed parts are used and/or variability caused by different sedimentation velocities of grated cheese particles with different size or densities during packaging operations.

NIR measurements applied to industrial grating operations showed differences both as a function of cheese batch and process time from the start of grating operations ($P < 0.05$); as reported in Fig. 5, no clear trends were observed in samples collected at different process times. A high variability was observed among grating operations carried out on different cheese batches, ranging from 9.19 ± 1.77% of batch 1 to 17.36 ± 1.68% of batch 7; this can be attributed to the variability that is obtained during the loading operations of both trimmed pieces of cheese and whole wheels that are addressed to the grater. Moreover, intra-treatment variability was also visible for some samples, as highlighted by samples standard deviation and can be caused by the reported error of PLS model based on NIR spectroscopy. The first six product batches amply fell within the rind limit content of 18%, except for batch 7 that was close to the limit. The NIR model here developed proved to rapidly provide an indication of rind percentage before the products are released in the market, allowing to further check and manage non-compliant products.

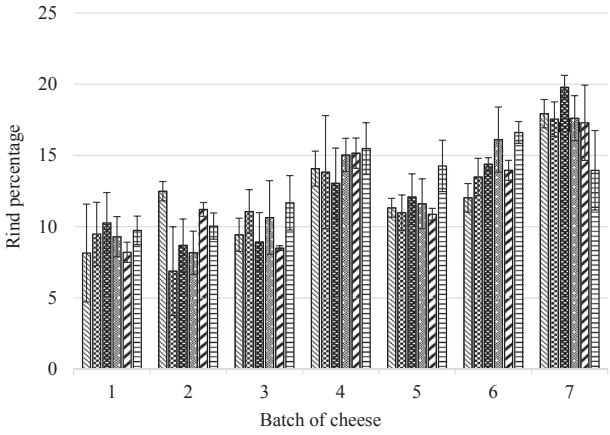

Fig. 5. Percentage of rind of grated Parmigiano-Reggiano cheese samples produced from 7 different grating processes and measured at 5 different process times, namely (left to right) T0 (▨), T1 (▩), T2 (▩), T3 (▩), T4 (▨), and T5 (▤) min.

4. Conclusions

This study enabled better understanding to be gained about the physical properties of grated P-R cheese, highlighting the different characteristics of cheese particles generated by the rind and by the inner part of the cheese; moreover, it was shown that these differences were highly related to the different texture and moisture content between the inner and the rind zone of the cheese.

PLS models built on selected sub-region of the NIR spectra to minimise water absorption bands, proved to successfully predict not only the rind content but also the particle size characteristics of grated P-R cheese and can be used to monitor the industrial grating process, with both inline and offline applications.

Image analysis was useful to study the physical characteristics of the cheese particles and allowed to develop PLS stable models to predict number of particles and total surface covered by the particles.

Both NIR and IA proved to be reliable tools that could be employed by grated P-R cheese producers as internal quality control measurements to efficiently comply with both PDO regulation and quality programs.

Acknowledgements

This study was partially founded by Nuova Castelli Spa (Reggio Emilia, Italy). The authors would like to thank Fabrizio Salvadorini and Roberto Pastorelli of Nuova Castelli Spa for their valuable contribution in the development of the work; furthermore, authors

want to thank Giovanni Cabassi and Stefana Barzaghi (CREA-ZA, Lodi, Italy) for the technical support and Marco Donatini and Davide Barosi for their help in the execution of the experimental measurements during their graduate studies.

References

AOAC. (1990). *Official methods of analysis of AOAC International* (15th ed., Vol. 1). Washington, DC, USA: AOAC International.

Barzaghi, S., Michelini, S., Cremonesi, K., Nocetti, M., Marinoni, L., & Cabassi, G. (2016). Uso della spettroscopia NIR per rilevare il contenuto di crosta in formaggio Parmigiano-Reggiano grattugiato. In *Atti del 7° simposio Italiano di spettroscopia NIR* (pp. 78–82). Milan, Italy.

Biasioli, F., Gasperi, F., Aprea, E., Endrizzi, I., Framondino, V., Marini, F., et al. (2006). Correlation of PTR-MS spectral fingerprints with sensory characterisation of flavour and odour profile of "Trentingrana" cheese. *Food Quality and Preference, 17*, 63–75.

Breuil, P., & Meullenet, J. F. (2001). A comparison of three instrumental tests for predicting sensory texture profiles of cheese. *Journal of Texture Studies, 32*, 41–55.

Brosnan, T., & Sun, D.-W. (2004). Improving quality inspection of food products by computer vision. *Journal of Food Engineering, 61*, 3–16.

Caccamo, M., Melilli, C., Barbano, D. M., Portelli, G., Marino, G., & Licitra, G. (2004). Measurement of gas holes and mechanical openness in cheese by image analysis. *Journal of Dairy Science, 87*, 739–748.

Campbell, G. M., Fang, C., & Muhamad, I. I. (2007). On predicting roller milling performance VI: Effect of kernel hardness and shape on the particle size distribution from first break milling of wheat. *Food and Bioproducts Processing, 85*, 7–23.

Cattaneo, S., Hogenboom, J. A., Masotti, F., Rosi, V., Pellegrino, L., & Resmini, P. (2008). Grated Grana Padano cheese: New hints on how to control quality and recognize imitations. *Dairy Science & Technology, 88*, 595–605.

Cevoli, C., Fabbri, A., Gori, A., Caboni, M., & Guarnieri, A. (2013). Screening of grated cheese authenticity by NIR spectroscopy. *Journal of Agricultural Engineering, 44*, 264–267.

Cevoli, C., Gori, A., Nocetti, M., Cuibus, L., Caboni, M. F., & Fabbri, A. (2013). FT-NIR and FT-MIR spectroscopy to discriminate competitors, non-compliance and compliance grated Parmigiano Reggiano cheese. *Food Research International, 52*, 214–220.

Cevoli, C., Ragni, L., Gori, A., Berardinelli, A., & Caboni, M. F. (2012). Quality parameter assessment of grated Parmigiano–Reggiano cheese by waveguide spectroscopy. *Journal of Food Engineering, 113*, 201–209.

Cevoli, C., Ragni, L., Iaccheri, E., Gori, A., Caboni, M. F., Guarnieri, A., et al. (2015). Estimation of the main compositional features of grated Parmigiano Reggiano cheese by a simple capacitive technique. *Journal of Food Engineering, 149*, 181–187.

Door. (2018). *DOOR agricultural and rural development. European Commission.* http://ec.europa.eu/agriculture/quality/door/list.html. (Accessed 29 October 2018).

Downey, G., Sheehan, E., Delahunty, C., O'Callaghan, D., Guinee, T., & Howard, V. (2005). Prediction of maturity and sensory attributes of Cheddar cheese using near-infrared spectroscopy. *International Dairy Journal, 15*, 701–709.

Du, Y. P., Liang, Y. Z., Jiang, J. H., Berry, R. J., & Ozaki, Y. (2004). Spectral regions selection to improve prediction ability of PLS models by changeable size moving window partial least squares and searching combination moving window partial least squares. *Analytica Chimica Acta, 501*, 183–191.

EU. (2012). Regulation (EU) No 1151/2012 of the European Parliament and of the Council on quality schemes for agricultural products and foodstuffs. *Official Journal of the European Union, 343*, 1–29.

Fang, C., & Campbell, G. M. (2003). On predicting roller milling performance IV: Effect of roll disposition on the particle size distribution from first break milling of wheat. *Journal of Cereal Science, 37*, 21–29.

Febbi, P., Menesatti, P., Costa, C., Pari, L., & Cecchini, M. (2015). Automated determination of poplar chip size distribution based on combined image and multivariate analyses. *Biomass and Bioenergy, 73*, 1–10.

Frake, P., Luscombe, C. N., Rudd, D. R., Gill, I., Waterhouse, J., & Jayasooriya, U. A. (1998). Near-infrared mass median particle size determination of lactose monohydrate, evaluating several chemometric approaches. *Analyst, 123*, 2043–2046.

Gerretzen, J., Szymańska, E., Bart, J., Davies, A. N., van Manen, H. J., van den Heuvel, E. R., et al. (2016). Boosting model performance and interpretation by entangling preprocessing selection and variable selection. *Analytica Chimica Acta, 938*, 44–52.

Haddad, Y., Mabille, F., Mermet, A., Abecassis, J., & Benet, J. C. (1999). Rheological properties of wheat endosperm with a view on grinding behaviour. *Powder Technology, 105*, 89–94.

Holroyd, S. E. (2013). The use of near infrared spectroscopy on milk and milk products. *Journal of Near Infrared Spectroscopy, 21*, 311–322.

Iezzi, R., Locci, F., Ghiglietti, R., Belingheri, C., Francolino, S., & Mucchetti, G. (2012). Parmigiano Reggiano and Grana Padano cheese curd grains size and distribution by image analysis. *LWT-Food Science and Technology, 47*, 380–385.

Jaster, H., Campos, A. C. L. P. D., Auer, L. B., Los, F. G. B., Salem, R. D. S., Esmerino, L. A., et al. (2014). Quality evaluation of parmesan-type cheese: A chemometric approach. *Food Science and Technology, 34*, 181–188.

Jiang, J. H., Berry, R. J., Siesler, H. W., & Ozaki, Y. (2002). Wavelength interval selection in multicomponent spectral analysis by moving window partial least-squares regression with applications to mid-infrared and near-infrared spectroscopic data. *Analytical Chemistry, 74*, 3555–3565.

Karoui, R., Dufour, E., & De Baerdemaeker, J. (2007). Front face fluorescence spectroscopy coupled with chemometric tools for monitoring the oxidation of semi-hard cheeses throughout ripening. *Food Chemistry, 101*, 1305–1314.

Karoui, R., Mouazen, A. M., Dufour, É., Pillonel, L., Schaller, E., De Baerdemaeker, J., et al. (2006). Chemical characterisation of European Emmental cheeses by near infrared spectroscopy using chemometric tools. *International Dairy Journal, 16*, 1211–1217.

Kennard, R. W., & Stone, L. A. (1969). Computer aided design of experiments. *Technometrics, 11*, 137–148.

Lindner, J. D. D., Bernini, V., De Lorentiis, A., Pecorari, A., Neviani, E., & Gatti, M. (2008). Parmigiano Reggiano cheese: Evolution of cultivable and total lactic microflora and peptidase activities during manufacture and ripening. *Dairy Science & Technology, 88*, 511–523.

Malacarne, M., Summer, A., Franceschi, P., Formaggioni, P., Pecorari, M., Panari, G., et al. (2009). Free fatty acid profile of Parmigiano–Reggiano cheese throughout ripening: Comparison between the inner and outer regions of the wheel. *International Dairy Journal, 19*, 637–641.

Mayer, H. K. (1996). Electrophoretic ripening index for the evaluation of proteolysis and the deduction of the age of Parmesan cheese. *Zeitschrift für Lebensmittel-Untersuchung und Forschung, 202*, 465–470.

Menesatti, P., Antonucci, F., Pallottino, F., Roccuzzo, G., Allegra, M., Stagno, F., et al. (2010). Estimation of plant nutritional status by Vis–NIR spectrophotometric analysis on orange leaves [*Citrus sinensis* (L) Osbeck cv Tarocco]. *Biosystems Engineering, 105*, 448–454.

Mucchetti, G., Gatti, M., Nocetti, M., Reverberi, P., Bianchi, A., Galati, F., et al. (2014). Segmentation of Parmigiano Reggiano dairies according to cheese-making technology and relationships with the aspect of the cheese curd surface at the moment of its extraction from the cheese vat. *Journal of Dairy Science, 97*, 1202–1209.

Musi, V., & Filippi, A. (2015). La tecnologia VIS-NIR online nel controllo del contenuto di crosta nel grattugiato di Parmigiano Reggiano. *Scienza e Tecnica Lattiero-Casearia, 66*, 107–110.

Ni, H., & Guansekaran, S. (2004). Image processing algorithm for cheese shred evaluation. *Journal of Food Engineering, 61*, 37–45.

Niu, X., Shen, F., Yu, Y., Yan, Z., Xu, K., Yu, H., et al. (2008). Analysis of sugars in Chinese rice wine by Fourier transform near-infrared spectroscopy with partial least-squares regression. *Journal of Agricultural and Food Chemistry, 56*, 7271–7278.

Parmigiano-Reggiano Consortium. (2017). *Rapporto annuale attività 2017.* https://www.parmigianoreggiano.it/comunicazione/rapporto_annuale_dell_attivita/default.aspx. (Accessed 29 October 2018).

Patel, H. G., Upadhyay, K. G., Miyani, R. V., & Pandya, A. J. (1993). Instron texture profile of buffalo milk Cheddar cheese as influenced by composition and ripening changes. *Food Quality and Preference, 4*, 187–192.

Shintu, L., & Caldarelli, S. (2005). High-resolution MAS NMR and chemometrics: Characterization of the ripening of Parmigiano Reggiano cheese. *Journal of Agricultural and Food Chemistry, 53*, 4026–4031.

Silaghi, F. A., Giunchi, A., Fabbri, A., & Ragni, L. (2009). Estimation of rheological properties of ice cream unfrozen liquid phase by FT-NIR spectroscopy. *Bulletin of the University of Agricultural Sciences and Veterinary Medicine, Cluj-Napoca Agriculture, 66*, 453–458.

Subramanian, A., & Rodriguez-Saona, L. (2009). Fourier transform infrared (FT IR) spectroscopy. In D.-W. Sun (Ed.), *Infrared spectroscopy for food quality analysis and control* (pp. 146–173). New York, NY, USA: Academic Press.

Sugimoto, K., Hashimoto, Y., Fukuike, C., Kodama, N., & Minagi, S. (2014). Image analysis of food particles can discriminate deficient mastication of mixed foodstuffs simulating daily meal. *Journal of Oral Rehabilitation, 41*, 184–190.

Zannoni, M. (2010). Evolution of the sensory characteristics of Parmigiano–Reggiano cheese to the present day. *Food Quality and Preference, 21*, 901–905.

Zannoni, M., & Hunter, E. A. (2015). Relationship between sensory results and compliance scores in grated Parmigiano-Reggiano cheese. *Italian Journal of Food Science, 27*, 487–494.

Zhu, Q., Xing, Y., Lu, R., Huang, M., & Ng, P. K. (2017). Visible/shortwave near infrared spectroscopy and hyperspectral scattering for determining bulk density and particle size of wheat flour. *Journal of Near Infrared Spectroscopy, 25*, 116–126.